Laser guiding of cold molecules in a hollow optical fiber and continuous-wave cold molecular beam generation*

Liu Run-Qin(刘润琴)[a)b)], Yin Ya-Ling(尹亚玲)[a)c)], and Yin Jian-Ping(印建平)[a)†]

[a)] *State Key Laboratory of Precision Spectroscopy, Department of Physics, East China Normal University, Shanghai* 200062, *China*

[b)] *Department of Physics, Kashgar Teachers College, Kashgar* 844008, *China*

[c)] *Department of Physics, National Laboratory of Solid State Microstructures, Nanjing University, Nanjing* 210093, *China*

(Received 7 January 2011; revised manuscript received 13 April 2011)

A novel scheme for guiding arbitrary buffer-gas cooled neutral molecules in a hollow optical fiber (HOF) using a red-detuned HE_{11} mode is proposed and analysed theoretically. We give the electromagnetic field distribution of the HE_{11} mode in the HOF and calculate the optical potential of an I_2 molecule, and study the molecule guiding mechanism using a classical Monte Carlo simulation. Using a 6 kW input laser, an S-shape HOF with a 2 cm curvature radius for both bends, and an input molecular beam with a transverse temperature of 0.5 K and longitudinal temperature of 5 K, we obtain a guiding efficiency of ∼0.126% for the scheme, and the transverse and longitudinal temperatures of the guided molecular beam are 1.9 mK and 0.5 K, respectively.

Keywords: laser guiding, cold molecular beam

PACS: 33.80.Gj, 37.10.Mn, 87.80.Cc **DOI:** 10.1088/1674-1056/21/3/033302

1. Introduction

Cold molecules have potential applications in cold molecular spectroscopy and accurate measurement,[1] molecular collision and cold chemistry,[2,3] quantum computing and quantum information processing,[4,5], and so on. As such, molecule decelerating,[6] trapping,[7,8] manipulating[9] and especially molecule guiding, have attracted more and more attention. In 2000 Loesch and Scheel[10] proposed and experimentally demonstrated the first electrostatic guide for cold polar molecules,[10] and in 2004 Junglen *et al.*[11] proposed and demonstrated an S-shape electrostatic guide. In 2007 Tsuji *et al.*[12] demonstrated a U-shape electrostatic guide, and Patterson *et al.*[13] a magnetic guide. Our group have also demonstrated two electrostatic guides.[14,15] However, all these guides are only applicable for polar molecules or paramagnetic molecules and cannot be used to guide molecules without a permanent electric or magnetic dipole moment. So it would be interesting and worthwhile to find a promising optical guide which can be used not only to guide molecules but also to produce an arbitrary cold molecular beam by bending it to a velocity filter. In the present paper, we propose a novel scheme to guide arbitrary buffer-gas cooled neutral molecules with a red-detuned HE_{11} mode in a hollow optical fiber (HOF), and obtain an optical velocity filter by bending the HOF to the S shape. The rest of the paper is organized as follows. In Section 2, we propose a scheme to guide cold molecules and calculate the optical potential for I_2 molecules. In Section 3, we perform a Monte Carlo simulation by using numerically integrating Newton's equations of motion with the Runge–Kutta method, and obtain the guiding efficiency, the transverse and longitudinal temperature, as well as the velocity profiles of the output molecular beam. In Section 4, some of the main results and a conclusion are summarized.

*Project supported by the National Natural Science Foundation of China (Grant Nos. 10804031, 10904037, 10434060, 10674047, 11034002, and 10904060), the National Basic Research Program of China (Grant Nos. 2006CB921604 and 2011CB921602), the Basic Key Program of Shanghai Municipality, China (Grant No. 07JC14017), the Shanghai Leading Academic Discipline Project, China (Grant No. B408), and the Jiangsu Provincial Projects for Postdoctoral Research Funds, China (Grant No. 0802009B).

†Corresponding author. E-mail: jpyin@phy.ecnu.edu.cn

© 2012 Chinese Physical Society and IOP Publishing Ltd

2. The guiding scheme and optical potential of the I_2 molecule in the HOF

2.1. The cold molecule guiding scheme

A scheme to guide cold molecules using a red-detuned HE_{11} Gaussian mode in a cylindrical HOF is shown in Fig. 1. The HOF is composed of a hollow region with radius a and a dielectric shell. As shown in Fig. 1(b), a red-detuned Gaussian beam (GB) with a vertical linear polarization is coupled into the hollow region of the HOF to excite the HE_{11} mode. At the same time, a continuous-wave (CW) molecular beam is injected into the HOF. The HE_{11} mode is azimuthally symmetric with the maximum intensity on the fiber axis and has almost zero intensity at the wall. Then, in the HOF, the molecules suffer the dipole force arising from their alternating current (AC) stark interaction with the optical field. As the laser beam is red-detuned, the molecules are attracted to the high-intensity region in the transverse direction, and are consequently guided through the fiber along the axis. The HOF is composed of two bends, and each bend has a curvature radius R and is followed by an approximately 20 cm-long straight guide (see Figs. 1(b) and 1(c)). In these two bends, the molecule suffers not only a dipole force but also an inertial centrifugal force, and the molecule with a large longitudinal velocity can then be rejected and lost. Like the evaporative cooling, the velocity distribution of the guided molecular beam can become narrower than that of the input beam. In this paper, the dielectric shell of the HOF is made of sapphire, whose complex refractive index at a wavelength of $\lambda = 10.6$ μm is $n = 0.67$–0.03i,[16] and the input laser is a CO_2 laser at $\lambda = 10.6$ μm.

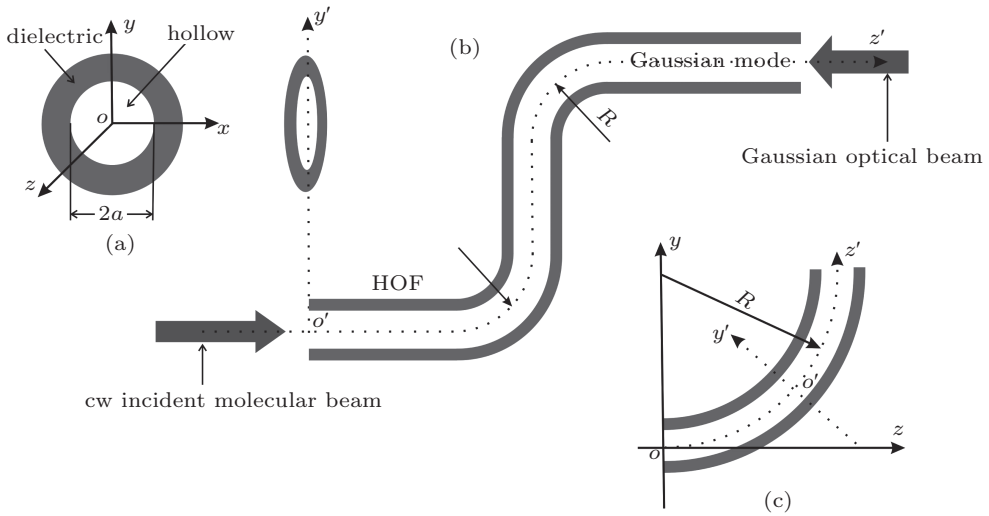


Fig. 1. (a) Structure of the HOF, (b) schematic diagram of the molecule guide, and (c) transformation of the two coordinates.

2.2. Intensity distribution and mode coupling of the HE_{11} mode

Since we use a Gaussian beam (GB) to excite the HOF, the lowest order HE_{11} hybrid mode (a Gaussian mode) in the cylindrical HOF will be excited selectively, while other modes cannot be efficiently excited (i.e. their coupling efficiencies are very low). The electromagnetic fields of the HE_{11} mode in the hollow region of the HOF ($E_{r11}^{\rm hollow}$, $E_{\varphi 11}^{\rm hollow}$, E_z; $H_{r11}^{\rm hollow}$, $H_{\varphi 11}^{\rm hollow}$, H_z) can be expressed in the cylindrical coordinate system (r, φ, z) as[17]

$$
\begin{aligned}
&E_{r11}^{\rm hollow} = {\rm J}_0\left(\frac{r}{a}u_{11}\right)\sin\varphi\,{\rm e}^{-\alpha_{11}z}\,{\rm e}^{{\rm i}(\beta_{11}z-\omega t)},\\
&E_{\varphi 11}^{\rm hollow} = {\rm J}_0\left(\frac{r}{a}u_{11}\right)\cos\varphi\,{\rm e}^{-\alpha_{11}z}\,{\rm e}^{{\rm i}(\beta_{11}z-\omega t)},\\
&E_z \to 0,\\
&H_{r11}^{\rm hollow} = -\sqrt{\frac{\varepsilon_0}{\mu_0}}{\rm J}_0\left(\frac{r}{a}u_{11}\right)\cos\varphi\;{\rm e}^{-\alpha_{11}z}\,{\rm e}^{{\rm i}(\beta_{11}z-\omega t)},\\
&H_{\varphi 11}^{\rm hollow} = \sqrt{\frac{\varepsilon_0}{\mu_0}}{\rm J}_0\left(\frac{r}{a}u_{11}\right)\sin\varphi\;{\rm e}^{-\alpha_{11}z}\,{\rm e}^{{\rm i}(\beta_{11}z-\omega t)},\\
&H_z \to 0,
\end{aligned}
\tag{1}
$$

where $J_0(x)$ is the zeroth-order Bessel function of the first kind, $u_{11} \approx 2.405$ is the geometrical mode factor

of the HE_{11} mode, a is the radius of the hollow region, ω is the angular frequency of the input laser, ε_0 and μ_0 are the vacuum dielectric constant and magnetic permeability, respectively, and α_{11} and β_{11} are the imaginary and the real parts of the axial propagation coefficient of the HE_{11} mode, respectively. The electromagnetic fields of the HE_{11} mode in the dielectric shell of the HOF are very small and are given by $E_{11}^{\text{dielectric}} \to 0$ and $H_{11}^{\text{dielectric}} \to 0$.

The intensity distribution of the HE_{11} mode in the HOF can be calculated by the longitudinal component of the time-averaged Poynting vector as[18]

$$I = \frac{A}{2}(E_{r11}^{\text{hollow}} \times H_{\varphi 11}^{\text{hollow}} - E_{\varphi 11}^{\text{hollow}} \times H_{r11}^{\text{hollow}}), \quad (2)$$

where A is a constant and can be calculated by the dependence of the propagating power P on the intensity distribution in the HOF,

$$P = \int_0^a I \times 2\pi r \mathrm{d}r. \quad (3)$$

From Eqs. (1)–(3), we can obtain

$$I = \frac{\mathrm{e}^{-2\alpha_{11}z} P \mathrm{J}_0^2\left(\frac{r}{a}u_{11}\right)}{\pi a^2[\mathrm{J}_0^2(u_{11}) + \mathrm{J}_1^2(u_{11})]}. \quad (4)$$

The coupling efficiency of the HE_{11} mode, i.e. the ratio of power P of the HE_{11} mode to the input power of the Gaussian beam, is given by[19]

$$C = \frac{\left|\int_0^a E^{\text{GB}}(r)\ \mathrm{J}_0\left(\frac{r}{a}u_{11}\right) r \mathrm{d}r\right|^2}{\int_0^\infty |E^{\text{GB}}(r)|^2\ r\,\mathrm{d}r\ \int_0^a \mathrm{J}_0^2\left(\frac{r}{a}u_{11}\right) r\,\mathrm{d}r}, \quad (5)$$

where $E^{\text{GB}}(r)$ is the electric field profile of the GB and can be described by

$$E^{\text{GB}}(r) = \frac{\sqrt{2P_{\text{in}}}}{w_0\sqrt{\pi}} \times \exp\left(-\frac{r^2}{w_0^2}\right), \quad (6)$$

P_{in} is the input power of the GB, and w_0 is the beam waist width of the GB.

Based on Eq. (5), we calculate the dependence of the coupling efficiency C of the HE_{11} mode on the beam waist of the incident GB and find that there is a maximum coupling efficiency for a given a (see Fig. 2). If we choose the beam waist of the GB to be $w_0 = 65.5$ μm and the inner radius of the HOF to be $a = 100$ μm, then coupling efficiency C of the HE_{11} mode can reach a maximum value of 98%, i.e. $P \approx 0.98P_{\text{in}}$, while the coupling efficiency for the other modes is only $\sim 2\%$.

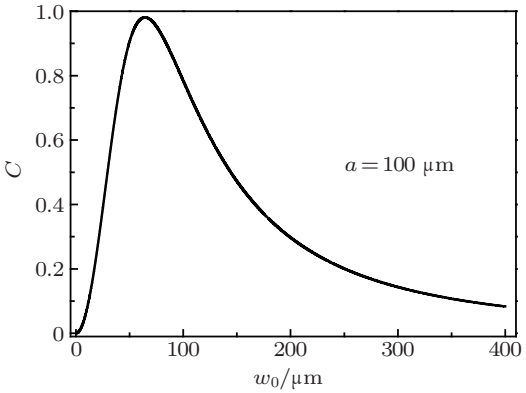


Fig. 2. The dependence of coupling efficiency C for the HE_{11} mode on beam waist w_0 of the incident Gaussian beam.

2.3. Propagation loss of the HE_{11} mode in HOF

In a straight HOF, the HE_{11} mode has an attenuation coefficient[17]

$$\alpha_{11\infty} = \left(\frac{u_{11}}{2\pi}\right)^2 \frac{\lambda^2}{a^3} \mathrm{Re}\left[\frac{n^2+1}{2\sqrt{n^2-1}}\right]. \quad (7)$$

And in a bend HOF, when the bending radius R is large, the HE_{11} mode has an attenuation coefficient proportional to $1/R^2$.[17] On the other hand, when the bending radius is much smaller than a critical radius R_u,[20] the attenuation coefficient of the HE_{11} mode is proportional to $1/R$.[21] In our case, we choose the inner radius to be $a = 100$ μm and the bend radius to be $R = 2$, 3, 4, 5, 6 cm, then the attenuation coefficient of the HE_{11} mode is

$$\alpha_{11}(R) = \frac{1}{R}\left[c_{\text{m}} \mathrm{Re}(z_{\text{TE}}) + c_{\text{s}} \mathrm{Re}(y_{\text{TM}})\right], \quad (8)$$

where $z_{\text{TE}} = \frac{1}{\sqrt{n^2-1}}$, $y_{\text{TM}} = \frac{n^2}{\sqrt{n^2-1}}$, $c_{\text{m}} = 1 - 0.231\frac{1}{\sqrt{b}} - 1.98\frac{1}{b} + 5.20\frac{1}{\sqrt{b^3}}$, $c_{\text{s}} = 0.570\frac{1}{\sqrt{b}} + 1.12\frac{1}{b} + 1.45\frac{1}{\sqrt{b^3}}$, $b = (n_0 k_0 a)^2\, a/R$, n_0 is the refractive index of air, and $k_0 = 2\pi/\lambda$ is the wave number in the vacuum for the input laser.

2.4. The optical potential of the I_2 molecule

When a molecule enters into the HOF, it will interact with the optical field due to the AC stark effect. The molecule has a Stark shift U (i.e. the optical potential) given by[22,23]

$$U = -\frac{\alpha}{2\varepsilon_0 c} I, \quad (9)$$

where α is the polarizability of the molecule, and c is the velocity of light. From Eqs. (4) and (9), we obtain

$$U = -\frac{\mathrm{e}^{-2\alpha_{11}z} P \alpha \mathrm{J}_0^2\left(\frac{r}{a}u_{11}\right)}{2c\pi\varepsilon_0 a^2[\mathrm{J}_0^2(u_{11}) + \mathrm{J}_1^2(u_{11})]}. \quad (10)$$

For an I_2 molecule, $\alpha = 12.1 \times 10^{-40}$ $C^2{\cdot}m^2{\cdot}J^{-1}$.[24] According to Eq. (10), we calculate the dependence of the optical potential of an I_2 molecule on radial position r for $a = 100$ μm, $\lambda = 10.6$ μm, $P = 6$ kW, and $z = 0$. As shown in Fig. 3, it is evident that the HE_{11} mode in the HOF is a Gaussian-shaped one, which can be used to guide cold molecules when the incident laser beam is red-detuned.

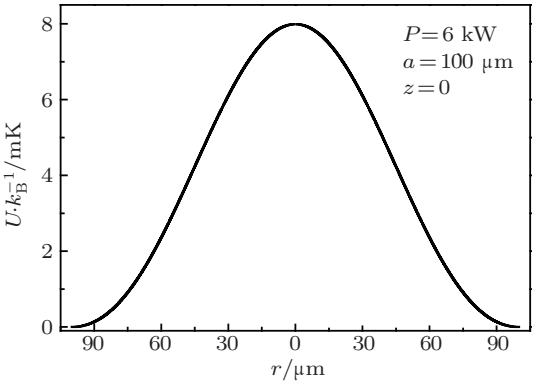


Fig. 3. The radial distribution of the optical potential for $z = 0$.

3. Monte Carlo simulation

3.1. The spatial and velocity distributions of the input molecular beam

In the following discussion, we assume that the incident molecular beam has a Gaussian transverse spatial distribution[11]

$$f(x,y) = \frac{1}{\pi w^2}\exp\left(-\frac{x^2+y^2}{w^2}\right), \tag{11}$$

a Gaussian transverse velocity distribution

$$f(v_x,v_y) = \frac{1}{\pi v_{\rm Tm}^2}\exp\left(-\frac{v_x^2+v_y^2}{v_{\rm Tm}^2}\right), \tag{12}$$

and a normalized longitudinal velocity distribution in the flux of the molecules

$$f(v_z) = \frac{2v_z}{v_{\rm Lm}^2}\exp\left(-\frac{v_z^2}{v_{\rm Lm}^2}\right), \tag{13}$$

where $v_{\rm Tm} = \sqrt{k_{\rm B}T_{\rm Tm}/M}$, $v_{\rm Lm} = \sqrt{2k_{\rm B}T_{\rm Lm}/M}$, $T_{\rm Tm}$ and $T_{\rm Lm}$ are the transverse and the longitudinal temperatures of the molecular beam, respectively, $k_{\rm B}$ is the Boltzmann constant, and w is the molecular beam waist width.

3.2. The reference frame for simulation

In order to simplify the simulation, we introduce a corresponding S-shape reference frame (see Figs. 1(b) and 1(c)). In this frame, the z' axis follows the centre of the HOF, and the x' or y' axes are perpendicular to the guide. The transformation between this reference frame and the Cartesian coordinate is given by[25−27]

$$\begin{aligned} x &= x', \\ y &= R\left[1-\cos\left(z'/R\right)\right] + y'\cos\left(z'/R\right), \\ z &= \left(R-y'\right)\sin\left(z'/R\right). \end{aligned} \tag{14}$$

The unit vectors ($\boldsymbol{e}_x$, $\boldsymbol{e}_y$, $\boldsymbol{e}_z$) of the old coordinate system are related to the new ones ($\boldsymbol{e}'_x$, $\boldsymbol{e}'_y$, $\boldsymbol{e}'_z$) by the following equations:

$$\begin{aligned} \boldsymbol{e}_x &= \boldsymbol{e}'_x, \\ \boldsymbol{e}_y &= \boldsymbol{e}'_y\cos\left(z'/R\right) + \boldsymbol{e}'_z\sin\left(z'/R\right), \\ \boldsymbol{e}_z &= -\boldsymbol{e}'_y\sin\left(z'/R\right) + \boldsymbol{e}'_z\cos\left(z'/R\right). \end{aligned} \tag{15}$$

From Eqs. (14) and (15), we obtain the acceleration of the molecule motion expressed in the new coordinates as

$$\begin{aligned} \boldsymbol{a} = {} & a_{x'}\boldsymbol{e}_{x'} + \left[a_{y'} + \frac{v_{z'}^2}{R}\right]\boldsymbol{e}_{y'} \\ & + \left[a_{z'} - \frac{2v_{y'}v_{z'}}{R}\right]\boldsymbol{e}_{z'}. \end{aligned} \tag{16}$$

3.3. Monte Carlo simulation

To understand the molecule guiding mechanism, we study the dynamic process of the guided molecules using the classic Monte Carlo simulation. In the simulation, we make some assumptions. First, we assume that the molecules are classical particles. Second, if a molecule hits the wall of the HOF, we consider it to be lost from the waveguide. Third, the transverse and the longitudinal degrees of freedom do not mix with each other, which is a good assumption when the bend radius is much larger than the inner radius of the HOF. We choose I_2 as the test molecule, and its trajectory is obtained by numerically integrating Newton's equations of motion using the Runge–Kutta method, which converges faster than the direct integration. The guided I_2 molecule in the HOF experience is an optical dipole gradient force, which can be given by

$$F_x = -\frac{\partial U}{\partial x}, \quad F_y = -\frac{\partial U}{\partial y}, \quad F_z = -\frac{\partial U}{\partial z}. \tag{17}$$

According to Eq. (16), the acceleration of the molecule motion in the HOF can be expressed as

$$a_x = \frac{F_x}{M}, \quad a_y = \frac{F_y}{M} - \frac{v_z^2}{R}, \quad a_z = \frac{F_z}{M} + \frac{2v_yv_z}{R}, \tag{18}$$

where M is the mass of the guided molecules, $R = R_{\rm bend}$ in the two bends, and $R = \infty$ in the straight sections of the HOF.

We used a homemade C++ program and a parallel-operation computer system composed of 64 CPUs to perform the Monte Carlo simulation, in which $\sim 10^6$ input molecules are moved quasi-continuously with a time step of $\Delta t = 10^{-8}$ s. When a molecule moves to the end of the HOF, we stop the simulation of the molecule and begin the simulation of the next molecule, thus every molecule has its own motion trajectory. Finally, we collect the molecules in the area of $0 \le r \le a$, while those molecules localized outside this area are considered to be lost.

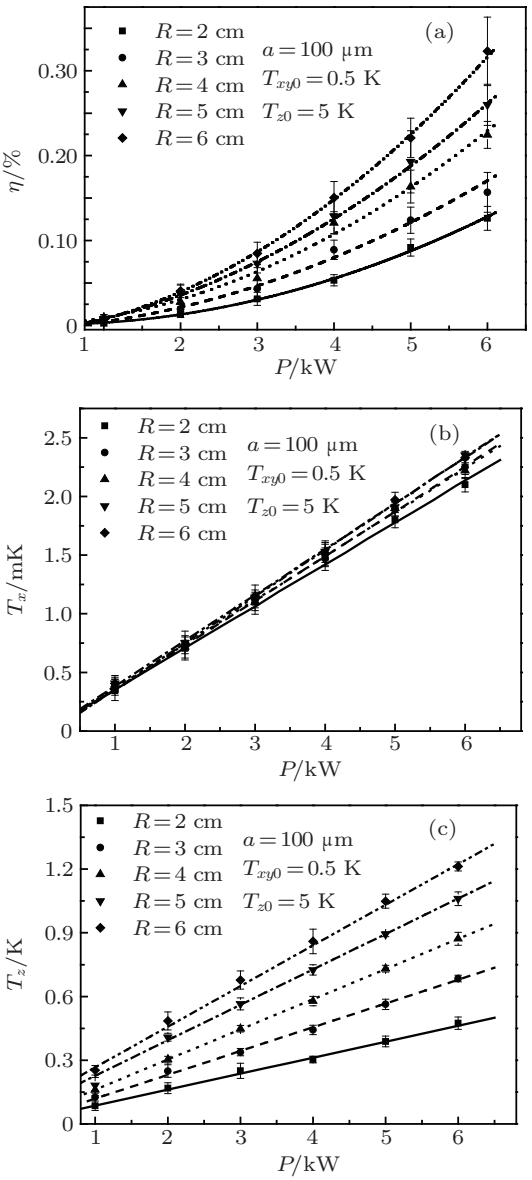


Fig. 4. The dependences of (a) the guiding efficiency, (b) the transverse temperature and (c) the longitudinal temperature of the guided molecular beam on laser power P and curvature radius R. The data points with error bars are the simulated results, and the curves are their corresponding fittings.

The dependences of the guiding efficiency, the transverse and the longitudinal temperatures of the guided molecular beam on input laser power P and curvature radius R are obtained from the Monte Carlo simulations. The data points with error bars are shown in Fig. 4. Every data point is simulated six times. We can see from Fig. 4 that the guiding efficiency, the longitudinal and the transverse temperatures of the guided molecular beam increase with the increase in input laser power and decrease with the reduction in curvature radius R. In particular, for $P = 6$ kW and $R = 2$ cm, the guiding efficiency of the guided molecular beam is $\sim 0.126\%$, which shows that a CW molecular beam with a flux of $10^8 \sim 10^9$ s^{-1} can be generated by our S-shaped HOF when the incident flux is about $10^{11} \sim 10^{12}$ s^{-1}.[13,28] The transverse and longitudinal temperatures of the guided molecular beam are about 1.9 mK and 0.5 K, respectively, which are much lower than those (0.5 K/5 K) of the input molecular beam due to the velocity filtering of the input molecules. Figure 5 shows the velocity distributions of the input molecular beam and the guided molecular beam for $P = 6$ kW and

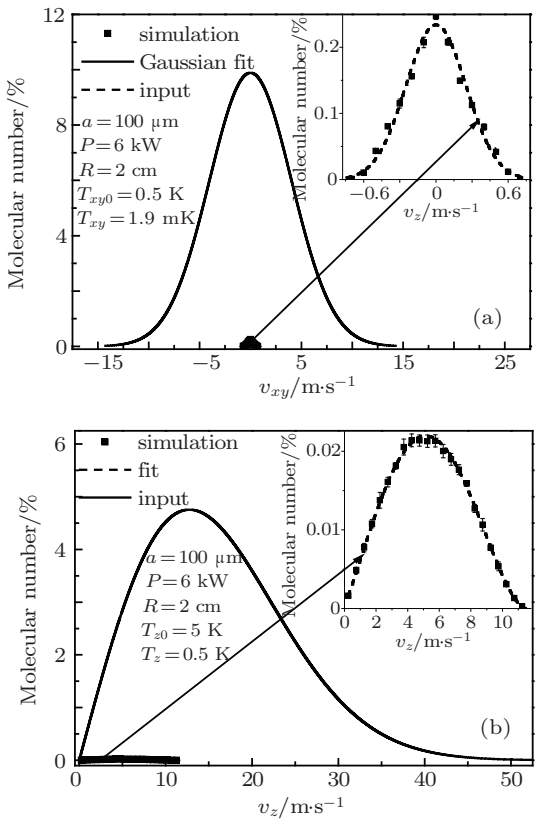


Fig. 5. (a) Transverse velocity and (b) longitudinal velocity distributions of the molecular beams. The inserts show the results of the guided molecular beams. The data points with error bars are the simulated results, the solid curves represent the normalized distributions of the input molecular beam, and the dotted curves (including the right inset) denote the corresponding fittings to the simulated results.

$R = 2$ cm. We can see from Fig. 5 that the transverse (Fig. 5(a)) and the longitudinal (Fig. 5(b)) velocity distributions of the guided beam have the same profiles as those of the input beam but are narrower and lower.

4. Conclusion

In this paper, we proposed a novel scheme to guide molecular beams using a red-detuned HE_{11} mode in the HOF. This scheme is applicable for arbitrary molecular beams. We calculated the optical potential of an I_2 molecule in the HOF and simulated the dependences of the guiding efficiency, the transverse and the longitudinal temperatures of the guided molecular beam on input laser power P and curvature radius R. In particular, when $P = 6$ kW and $R = 2$ cm, a CW molecular beam with a transverse temperature of 1.9 mK, a longitudinal temperature of 0.5 K and a molecular flux of $10^8 \sim 10^9$ s^{-1} can be generated. Such a guided cold molecular beam can be used in many research areas, such as optical Stark deceleration,[29,30] frequency standards,[31] cold molecular physics and optics, cold molecular spectroscopy, and cold molecular chemistry,[32] thus enriching neutral molecule manipulation and control. Moreover, our optical guiding scheme offers not only an effective method of generating a CW cold molecular beam, but also a novel technique for forming various molecule-optical devices, such as molecular funnels, molecular beam splitters and molecular interferometers.

References

[1] Hudson J J, Sauer B E, Tarbutt M R and Hinds E A 2002 *Phys. Rev. Lett.* **89** 023003

[2] Gilijamse J J, Hoekstra S, van de Meerakker S Y T, Groenenboom G C and Meijer G 2006 *Science* **313** 1617

[3] Hudson E R, Ticknor C, Sawyer B C, Taatjes C A, Lewandowski H J, Bochinski J R, Bohn J L and Ye Jun 2006 *Phys. Rev.* A **73** 063404

[4] DeMille D 2002 *Phys. Rev. Lett.* **88** 067901

[5] André A, DeMille D, Doyle J M, Lukin M D, Maxwell S E, Rabl P, Schoelkopf R J and Zoller P 2006 *Nat. Phys.* **2** 636

[6] Bethlem H L, Berden G and Meijer G 1999 *Phys. Rev. Lett.* **83** 1558

[7] Bethlem H L, Berden G, Crompvoets F M H, Jongma R T, van Roij A J A and Meijer G 2000 *Nature* **406** 491

[8] Zhou Q, Lu J F and Yin J P 2010 *Chin. Phys.* B **19** 123203

[9] Zhou Q, Lu J F and Yin J P 2010 *Chin. Phys.* B **19** 093202

[10] Loesch H J and Scheel B 2000 *Phys. Rev. Lett.* **85** 2709

[11] Junglen T, Rieger T, Rangwala S A, Pinkse P W H and Rempe G 2004 *Eur. Phys. J.* D **31** 365

[12] Tsuji H, Okuda Y, Sekiguchi T and Kanamori H 2007 *Chem. Phys. Lett.* **436** 331

[13] Patterson D and Doyle J M 2007 *J. Chem. Phys.* **126** 154307

[14] Xia Y, Yin Y, Chen H, Deng L and Yin J 2008 *Phys. Rev. Lett.* **100** 043003

[15] Liu Y, Yun M, Xia Y, Deng L and Yin J 2010 *Phys. Chem. Chem. Phys.* **12** 745

[16] Harrington J A and Christopher C G 1990 *Opt. Lett.* **15** 541

[17] Marcatili E A J and Schmeltzer R A 1964 *Bell Syst. Tech. J.* **43** 1783

[18] Ito H, Sakaki K, Nakata T, Jhe W and Ohtsu M 1995 *Opt. Commun.* **115** 57

[19] Saito M, Sato S and Miyagi M 1993 *J. Opt. Soc. Am.* A **10** 277

[20] Miyagi M 1981 *Appl. Opt.* **20** 1221

[21] Miyagi M, Harada K, Aizawa Y and Kawakami S 1984 *Proc. Soc. Photo-Opt. Instrum. Eng.* **484** 117

[22] Stapelfeldt H, Sakai H, Constant E and Corkum P B 1997 *Phys. Rev. Lett.* **79** 2787

[23] Sakai H, Tarasevitch A, Danilov J, Stapelfeldt H, Yip R W, Ellert C, Constant E and Corkum P B 1998 *Phys. Rev.* A **57** 2794

[24] Barker P F and Shneider M N 2002 *Phys. Rev.* A **66** 065402

[25] Renn M J, Zozulya A A, Donley E A, Cornell E A and Anderson D Z 1997 *Phys. Rev. A* **55** 3684

[26] Liu R, Zhou Q, Yin Y and Yin J 2009 *J. Opt. Soc. Am.* B **26** 1076

[27] Li D J, Hu Z F and Li S Q 2003 *Chin. Phys.* **12** 738

[28] Patterson D, Rasmussen J and Doyle J M 2009 *New J. Phys.* **11** 055018

[29] Yin Y, Zhou Qi, Deng L, Xia Y and Yin J 2009 *Opt. Express* **17** 10706

[30] Yin Y L, Xia Y and Yin J P 2008 *Chin. Phys.* B **17** 3672

[31] Bethlem H L, Kajita M, Sartakow B, Meijer G and Ubachs W 2008 *Eur. Phys. J.* ST **163** 55

[32] Willitsch S, Bell M T, Gingell A D, Procter S R and Softley T P 2008 *Phys. Rev. Lett.* **100** 043203